

# X-RAY LINES AND ABSORPTION EDGES IN GRBS AND THEIR AFTERGLOWS

M. Böttcher<sup>1</sup>

<sup>1</sup>*Department of Physics and Astronomy, Ohio University, Athens, OH 45701, USA*

## ABSTRACT

Absorption and Reprocessing of Gamma-ray burst radiation in the environment of cosmological GRBs can be used as a powerful probe of the elusive nature of their progenitors. In particular, transient X-ray emission line and absorption features in the prompt and early afterglows of GRBs are sensitive to details of the location and density structure of the reprocessing and/or absorbing material. To date, there have been only rather few detections of such features, and the significance is marginal in most individual cases. However, transient X-ray emission lines in GRB afterglows have now been found by four different X-ray satellites, which may justify a more detailed theoretical investigation of their origin. In this paper, I will first present a brief review of the status of observations of transient X-ray emission line and absorption features. I will then discuss general physics constraints which those results impose on isotropy, homogeneity, and location of the reprocessing material with respect to the GRB source, and review the various currently discussed, specific models of GRBs and their environments in which the required conditions could arise.

## SUMMARY OF OBSERVED X-RAY LINES AND ABSORPTION FEATURES

The precise localization of gamma-ray bursts (GRBs) by the BeppoSAX satellite, launched in 1996, has facilitated the subsequent discovery of X-ray and optical GRB afterglows, the measurement of redshifts of GRBs and the firm establishment of their cosmological distance scale (at least for long GRBs with durations  $t_{90} \gtrsim 2$  s) beyond any reasonable doubt. The physics of the radio through X-ray continuum afterglow emission are now believed to be rather well understood in terms of the external synchrotron shock model (for a recent review see, e.g., Mészáros 2002 or Dermer 2002). However, in spite of these significant advances, the ultimate source of GRBs is still a matter of vital debate. This is mainly due to the fact that the continuum GRB afterglows are the “smoking gun” of the GRB explosion, revealing only very little information about the initial energy source.

However, even without a direct observation of the central engines of GRBs, it might be possible to infer their nature indirectly if detailed probes of the structure and composition of their immediate vicinity can be found. A promising candidate for such a probe is high-quality, time resolved X-ray spectroscopy of GRB afterglows, which is now becoming available with the new generation of X-ray telescopes like *Chandra* and *XMM-Newton*, and the planned Swift mission, scheduled for launch in September 2003. Previous and currently operating X-ray telescopes have so far (status: November 2002) revealed marginal evidence for X-ray emission lines (mostly consistent with Fe  $K\alpha$  fluorescence lines) or radiative recombination edges in 5 GRBs, and one case of a transient X-ray absorption feature at an energy consistent with an iron K absorption edge.

In the remainder of this section, I will give a brief review of the observed X-ray spectral features in GRBs, before I turn to the implications of those observations in general terms. This will be followed by a summary of the currently discussed GRB models which could give rise to the conditions required to produce the observed spectral features.

### X-ray emission lines in GRB afterglows

Marginal evidence for transient X-ray emission line features in GRB afterglows have been reported for 5 Gamma-ray bursts: GRB 970508 (Piro et al. 1999), GRB 970828 (Yoshida et al. 2000), GRB 991216 (Piro et al. 2000), GRB 000214 (Antonelli et al. 2000), and 011211 (Reeves et al. 2002a). Tab. 1 lists the key observational features of these five GRB line detections: (1) the GRB identification, (2) the redshift, (3) the time interval of the respective line detection, (4) the isotropic luminosity of the emission line, (5) the instrument with which the detection was made, (6) additional remarks concerning the line detection, and (7) the reference to the detection and important contributions through re-analysis of the respective observations. Note that the beginning of the time intervals listed in column (3) are generally set by the beginning of the respective observations and might thus not be representative of the onset of the line emission.

Table 1. Observed X-ray emission line features in GRB afterglows.  $t_{\text{line}}$  is the time interval after the GRB trigger during which the respective feature(s) has (have) been detected.  $L_{\text{line}}$  is the luminosity in the respective emission line, assuming that the line emission is isotropic.

GRB	$z$	$t_{\text{line}}[\text{s}]$	$L_{\text{line}}[\text{ergs s}^{-1}]$	Instrument	Remarks	Reference(s)
970508	0.835	$2 \cdot 10^4$ $-5.6 \cdot 10^4$	$6 \cdot 10^{44}$	BeppoSAX	Sec. outburst at time of line detection  Line width in- consistent with photoionization	Piro et al. (1999)  Paehrels et al. (2000)
970828	0.958  (0.33)	$1.2 \cdot 10^5$ $-1.4 \cdot 10^5$	$5 \cdot 10^{44}$  ( $5 \cdot 10^{43}$ )	ASCA	Rad. rec. cont. without line ( $\leftarrow$ if em. feature is in- terpreted as Fe $K\alpha$ line)	Yonetoku et al. (2001) Yoshida et al. (1999)
991216	1.00	$1.3 \cdot 10^5$ $-1.5 \cdot 10^5$	$8 \cdot 10^{44}$	Chandra ACIS-S + HETG	Broad line + Rad. Rec. Cont. $\sigma_L \sim 0.23$ keV $\implies$ high velocity outflow $v \sim 0.1$ c	Piro et al. (2000)
000214	0.47	$4 \cdot 10^4$ $-1.5 \cdot 10^5$	$4 \cdot 10^{43}$	BeppoSAX	No optical transient; $z$ based on X-ray line	Antonelli et al. (2000)
011211	2.14	$4.0 \cdot 10^4$ $-6.7 \cdot 10^4$	Si XIV: $6.4 \cdot 10^{44}$ S XVI: $6.2 \cdot 10^{44}$ Ar XVIII: $4.4 \cdot 10^{44}$ Ca XX: $2.5 \cdot 10^{44}$	XMM- Newton	No iron line; reality of line detection con- troversial	Reeves et al. (2002a,b) Borozdin & Tru- dolyubov (2002)

In the *BeppoSAX* NFI observation of the afterglow of GRB 970508, Piro et al. (1999) detected evidence, at the  $\sim 3\sigma$  level, for an emission line feature consistent with a 6.7 keV Fe  $K\alpha$  line from highly ionized iron, at the redshift of the burst at  $z = 0.835$ . The X-ray afterglow of this burst exhibited a secondary outburst after  $\sim 6 \times 10^4$  s, and the disappearance of the line from the X-ray spectrum seemed to be coincident with the onset of this secondary X-ray outburst (Piro et al. 1999). Paehrels et al. (2000) re-analyzed the NFI spectrum containing the line. Fitting the spectrum with a plasma emission model in photoionization equilibrium, assuming an illuminating continuum identical to the GRB afterglow emission, they found that such a fit would either require too large a redshift, inconsistent with the redshift of the burst, or too high a temperature, inconsistent with the a priori assumption of the ionization state of the line-emitting medium

being dominated by photoionization. Paehrels et al. (2000) interpreted this inconsistency as possible evidence for thermal plasma emission rather than emission from a photoionized plasma.

Interestingly, the second GRB for which evidence for an X-ray emission feature in the redshifted Fe  $K\alpha$  energy regime was found, appears to be opposite in that respect. Before the redshift of GRB 970828 could be determined, Yoshida et al. inferred a redshift of  $z = 0.33$  from the energy of the line feature in the *ASCA* spectrum of the afterglow of this GRB, assuming that it corresponds to an Fe  $K\alpha$  line at 6.4 keV in the burst rest frame. In a later re-analysis, after the likely host-galaxy identification of GRB 970828, associated with a redshift of  $z = 0.958$  (Djorgovski et al. 2001), Yoshida et al. (2001) and Yonetoku et al. (2001) argued that the emission feature is consistent with this redshift if it is a radiative recombination continuum (RRC) edge rather than a fluorescence or recombination line. They argue that the electron temperature in the plasma responsible for the emission feature is inconsistent with the ionization temperature in thermal equilibrium, and would therefore indicate photoionization as the dominant ionization mechanism.

Marginal evidence for a RRC was also reported for the *Chandra* ACIS-S+HETG spectrum of the afterglow of GRB 991216 (Piro et al. 2000). Piro et al. (2000) interpret the width and the apparently blue-shifted best-fit energy of the iron line with respect to the redshift of the host galaxy at  $z = 1.00$  as the signature of a directed outflow velocity of  $v \sim 0.1c$  of the source of the recombination line and the RRC. If this interpretation is correct, it might be indicative of a supernova explosion a few months prior to the GRB.

For GRB 000214, no optical counterpart could be identified. In this case, the only information concerning its redshift comes from the X-ray emission line detected by the *BeppoSAX* NFI, and was estimated to be  $z = 0.47$ , if the emission line at  $E = (4.7 \pm 0.2)$  keV is interpreted as the redshifted Fe  $K\alpha$  line from hydrogen-like iron (Antonelli et al. 2000).

Recently, Reeves et al. (2002a,b) reported the marginal detection of a set of emission lines in the *XMM-Newton* spectrum of the early afterglow of GRB 011211. If real, these features would be peculiar in that they show evidence for  $K\alpha$  lines from the hydrogen-like ions of lighter elements, such as Si XIV, S XVI, Ar XVIII, and CA XX, but no indication of an Fe  $K\alpha$  line or RRC edge. Those lines appear to be blue-shifted by an average of  $v \sim 0.1c$  with respect to the likely redshift of the burst,  $z = 2.14$ . Reeves et al. (2002b) find that the addition of the low-Z metal line system to a pure power-law fit to the *XMM-Newton* EPIC-pn spectrum improves the  $\chi^2/d.o.f.$  from 51.5/28 to 21.9/22. However, Borozdin & Trudolyubov (2002) have pointed out several caveats of the tentative line detections in GRB 011211. (1) The set of low-Z metal emission lines appeared only in the first  $\sim 5$  ksec, prior to a re-pointing of the *XMM-Newton* spacecraft. During that time, the source was located very close to the edge of the CCD chip of the EPIC-pn detector. Repeating the analysis of Reeves et al. (2002a), but excluding 22 % of the counts from the immediate vicinity of the chip edge, they found that the significance of the lines dropped disproportionately. (2) Evidence for the lines appears only in the EPIC-pn detector, with no such indication in the EPIC-MOS detectors. (3) The measured centroid energy of the most prominent line at  $E = 0.70 \pm 0.02$  keV (attributed to Si XIV by Reeves et al. 2002b), is coincident with a line in the background from a region on the chip in the immediate vicinity of the edge. (4) In their analysis, Borozdin & Trudolyubov (2002) find the *XMM-Newton* spectrum of GRB 011211 consistent with a pure power law, with no evidence for spectral evolution in consecutive time intervals. The addition of an emission line system lowers the reduced  $\chi^2$  from 1.03 to 0.82 (with 8 additional free parameters), which might be an indication of over-fitting, rather than a statistically significant improvement of the fit.

### The Transient Absorption Feature in GRB 990705

Atomic X-ray absorption features in GRB afterglows are rather common. However, in order to distinguish such features from foreground absorption and to associate them physically with the GRB, one needs to find evidence for variability of those absorption features on the GRB / early afterglow time scale (Perna & Loeb 1998, Böttcher et al. 1999). Until now, only one such case has been observed: GRB 990705 (Amati et al. 2000). In this burst, a transient absorption feature has been found at  $(3.8 \pm 0.3)$  keV, consistent with an Fe K absorption edge from neutral iron at  $z = 0.86 \pm 0.17$  at the redshift of the host galaxy at  $z = 0.84$  (Lazzati et al. 2001). This absorption edge was only seen in the first 13 s of the GRB, while no evidence for excess absorption was found in later segments of the *BeppoSAX* WFC observations. The best fit to the segment with the most significant detection of the absorption edge (6 – 13 sec.), assuming an underlying

power-law absorbed by a neutral absorbing column  $N_H$  with solar abundances and an additional absorption edge yielded a depth of the absorption feature of  $\tau = 1.4 \pm 0.4$  and  $N_H = (3.5 \pm 1.4) \times 10^{22} \text{ cm}^{-2}$ . Leaving the iron abundance in the neutral absorber as a free parameter in a power-law fit to the spectrum in this time segment resulted in  $N_H = (1.32 \pm 0.3) \times 10^{22} \text{ cm}^{-2}$  and a relative overabundance of iron with respect to solar abundances of  $X_{\text{Fe}} = 75 \pm 19$ . Implications and possible interpretations of these results will be discussed in the final section of this review.

## GENERAL CONSTRAINTS FROM EMISSION LINE FEATURES

Analytic estimates of the fluorescence and/or recombination line emission in photoionized media in GRB environments have been presented by many authors (e.g., Mészáros & Rees 1998, Ghisellini et al. 1999, Lazzati et al. 1999, Böttcher 2000). A very general estimate of the amount of iron required to produce the observed iron line features can be derived from considering that in the course of complete photoionization of iron, on average  $\sim 5$  Fe  $K\alpha$  photons are emitted, since it takes on average  $\sim 12$  X-ray photons to ionize an initially neutral iron atom completely (taking into account the Auger effect), and the  $K\alpha$  fluorescence yield is in the range  $0.3 - 0.4$  for the various ionization stages of iron. In dilute media, if recombination is negligible, it would then take  $N_{\text{Fe}} \sim 2 \times 10^{56} L_{44} t_5$  iron atoms to produce an iron line of isotropic luminosity  $L_{\text{line}} = 10^{44} L_{44} \text{ ergs s}^{-1}$  over a time scale of  $\Delta t = 10^5 t_5 \text{ s}$ . If recombination and multiple ionization of the same iron atom enhance the efficiency of line production, one can introduce an enhancement factor  $f$ , counting the number of times that a single iron atom can effectively contribute 5  $K\alpha$  photons in the process of repeated cycles of ionization and recombination. One then arrives at a general estimate of

$$M_{\text{Fe}} \approx 0.16 \frac{L_{44} t_5}{f} M_{\odot} \quad (1)$$

In dilute, extended media, where recombination is inefficient,  $f \sim 1$ , while in dense media with efficient recombination,  $f \gg 1$ . Due to light travel time effects, the duration of the line emission will be at least  $t_{\text{line}} > R(1+z)(1 - \cos \theta_{\text{obs}})/c$ , where  $R$  is the extent of the reprocessing material. Thus, the size limit, together with the restriction that in the GRBs with line detections, there is no indication for excess X-ray absorption, leads to typical mass estimates of  $M_{\text{Fe}} \sim 0.1 - 1 M_{\odot}$  of iron, confined in  $R \lesssim 10^{-3} \text{ pc}$ , if the line emission were to originate in a dilute, quasi-isotropic environment. This is unlikely to be realized in any astrophysical setting, and may thus be ruled out (Ghisellini et al. 1998, Böttcher et al. 1999). We therefore find that inhomogeneous media with significant density enhancement outside our line of sight toward the GRB source are required (e.g., Lazzati et al. 1999, Böttcher 2000).

At this point, several geometries and general scenarios will have to be distinguished. First, the duration  $t_{\text{line}}$  of the line detection can be set either by the light travel time effect, which puts the reprocessor at distances of  $10^{15} \text{ cm} \lesssim R \lesssim 10^{16} \text{ cm}$ . These types of configurations are referred to as *distant reprocessor models*. Alternatively, the duration of the line emission can be determined by the duration of the illumination by a more persistent, gradually decaying central source. In that case, the reprocessor can be located much closer to the source than in the case of the distant reprocessor models. For this reason, these scenarios are referred to as *nearby reprocessor models* (see fig. 1). Second, we need to distinguish between different mechanisms ionizing the line-emitting iron atoms. The scenarios considered above are generally based on photoionization being the dominant ionization mechanism. However, it is very well conceivable that the material in the vicinity of GRBs is energized by shocks associated with the GRB explosion, and heated to temperatures of  $T \sim 10^7 - 10^8 \text{ K}$  (e.g., Vietri et al. 1999). In this case, and for sufficiently high densities, collisional ionization may dominate over photoionization, and the iron  $K\alpha$  line emission will be dominated by the recombination lines of H and He-like iron, accompanied by a radiative recombination continuum. We will refer to these models as “thermal models”, as opposed to the “photoionization models” mentioned above.

## PHOTOIONIZATION MODELS

General parameter studies on photoionization models have been done by many authors. An important complication keep in mind is the fact that the continuum illuminating the reprocessing material might not be identical or even similar to the observed afterglow emission. Most importantly, if the reprocessor is located at a distance of  $R = 10^{15} R_{15} \text{ cm}$ , and illuminated by GRB (and early afterglow) emission from a

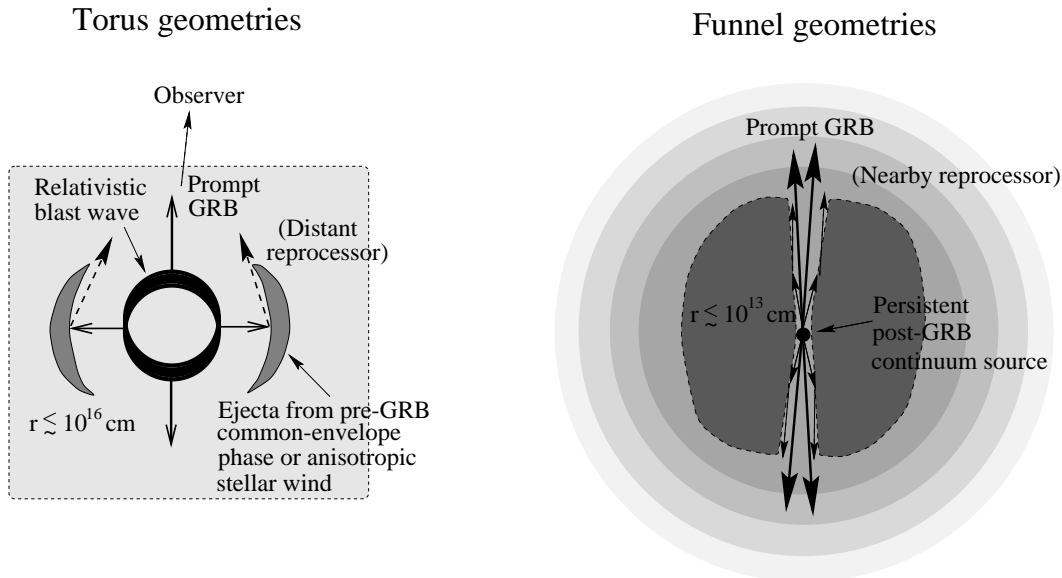


Fig. 1. Fundamental geometries of distant reprocessors (left) and nearby reprocessors (right).

relativistic blast wave advancing at a coasting speed corresponding to  $\Gamma = 100\Gamma_2$ , then it will be swept up by the blast wave after a typical illumination time of

$$t_{\text{ill}} \sim 2 \frac{R_{15}}{\Gamma_2^2} \text{ s} \quad (2)$$

unless the blast wave deceleration radius  $r_{\text{dec}} = 5 \times 10^{16} (E_{52}/n_0 \Gamma_2^2)^{1/3}$  cm is much less than  $10^{15}$  cm. Here,  $E_{52}$  is the isotropic equivalent energy of the GRB explosion in units of  $10^{52}$  ergs  $\text{s}^{-1}$  and  $n_0$  is the density of the (homogeneous) surrounding medium in units of  $\text{cm}^{-3}$ . The condition  $r_{\text{dec}} \ll 10^{15}$  cm would require a very low explosion energy directed toward the reprocessor, a large density of the decelerating external medium, and/or a very high bulk Lorentz factor  $\Gamma$ , i. e. a very low baryon contamination.

General studies of the reprocessing efficiency and spectral and temporal signatures of reprocessor models for X-ray emission lines in GRB environments (e.g., Ballantyne & Ramirez-Ruiz 2001, Lazzati et al. 2002, Ghisellini et al. 2002, Kallman et al. 2002) have yielded very useful insight into the general properties of such reprocessing features. The above caveat needs to be taken into account very carefully when applying these results to real GRBs and scaling illuminating spectra, ionization parameters etc., to properties derived from observed continuum afterglows of GRBs.

In a parameter-independent study, Lazzati et al. (2002) have calculated the efficiency of reprocessing a given ionizing flux into fluorescence and/or recombination line flux as a function of ionization parameter. This efficiency is generally at most  $\sim 1\%$  and dependent on the precise spectral shape of the illuminating spectrum. This implies that the observed iron lines listed in Tab. 1 require a total energy in the ionizing continuum of at least  $\sim 10^{51}$  ergs (Ghisellini et al. 2002). The reprocessing efficiency is drastically decreasing for high ionization parameters  $\xi \gtrsim 10^3$ . Lazzati et al. (2002) suggest that this may provide a diagnostic between distant and nearby reprocessor models.

Another important aspect associated with iron  $K\alpha$  line emission is related to radioactive decay of  $^{56}\text{Ni} \rightarrow ^{56}\text{Co} \rightarrow ^{56}\text{Fe}$  in the ejecta of a supernova which may be associated with the GRB (Lazzati et al. 2001, McLaughlin et al. 2002, McLaughlin & Wijers 2002). Since it is primarily  $^{56}\text{Ni}$  that is produced in the final stages of a supernova progenitor, any emission line features should gradually shift in energy from 8 keV for Nickel to 7.4 keV for Cobalt and 6.9 keV for hydrogen-like iron on the radioactive decay time scales of 6.1 d and 78.8 d for  $^{56}\text{Ni}$  and  $^{56}\text{Co}$ , respectively. However, McLaughlin et al. (2002) and McLaughlin & Wijers (2002) point out the curious detail that  $^{56}\text{Ni}$  would usually predominantly decay via electron capture. Thus,

if the reprocessing material happens to be highly ionized, the decay time scale may be significantly delayed w.r.t. the standard decay of neutral  $^{56}\text{Ni}$ . Consequently, for detailed modeling of the “iron” line emission in GRB afterglows, a rest-frame line energy of  $\sim 8$  keV might actually be a more appropriate assumption than the standard value of 6.4 – 6.97 keV. In the remainder of this review, I will, for simplicity, continue to refer to any line feature around  $E \sim 7$  keV in the GRB rest frame as “iron line”, keeping in mind that it might have a significant contribution from Ni and Co.

In addition to light-travel time effects, standard constraints on reprocessor models are obtained considering the ionization and recombination time scales. The ionization time scale may be estimated as

$$t_{\text{ion}} \approx \frac{12}{\int_{E_{\text{thr}}}^{\infty} \Phi_{\text{ion}}(E) \sigma_{\text{pi}}(E) dE} \approx \frac{12(\alpha + 2)}{\sigma_0 \Phi_0 E_{\text{thr}}}, \quad (3)$$

where  $E_{\text{thr}}$  is the photoionization threshold energy,  $\sigma_{\text{pi}}(E) \approx \sigma_0 (E/E_{\text{thr}})^{-3}$  is the photoionization cross section, and  $\Phi(E) = \Phi_0 (E/E_{\text{thr}})^{-\alpha}$  is the ionizing photon flux, assumed to be a straight power-law above the ionization threshold. Appropriate averages for the various ionization stages of iron are  $E_{\text{thr}} \sim 8$  keV and  $\sigma_0 \sim 3.5 \times 10^{20} \text{ cm}^{-2}$ . The recombination time scale can be approximated as

$$t_{\text{rec}} = \frac{1}{n_e \alpha_{\text{rec}}} \approx \frac{10^9 T_4^{3/4}}{n_H (Z_{\text{eff}}/26)^2} \text{ s}, \quad (4)$$

where  $\alpha_{\text{rec}}$  is the recombination coefficient,  $Z_{\text{eff}}$  is the effective nuclear charge,  $T_4$  is the electron temperature in units of  $10^4$  K, and  $n_H$  is the hydrogen number density in units of  $\text{cm}^{-3}$ . The approximation for the recombination rate used above assumes that recombination is dominated by radiative recombination, which becomes inaccurate for ionization states lower than Fe XXV at temperatures above  $\sim 10^5$  K.

Additional model constraints are derived from considerations concerning optical-depth effects due to resonance scattering out of the line of sight (for the resonant Ly $\alpha$  line of Fe XXVI) and Thomson scattering, which define a maximum depth in the reprocessor beyond which the material will effectively no longer contribute to the line emission.

### Distant Reprocessor Models

Distant reprocessor models, in which the duration of the line emission is dominated by the light travel time difference,  $t_{\text{line}} \sim R(1+z)(1 - \cos \theta_{\text{obs}})/c$ , were the first to be discussed after it became clear that quasi-isotropic fluorescence line emission scenarios were infeasible to explain the observed iron line features (e.g., Lazzati et al. 1999, Böttcher 2000). Generally, in these models, a photoionizing continuum from the central source, emitted in tandem with the prompt and early afterglow radiation, is impinging on a torus of dense, pre-ejected material. Recall, however, that the ionizing continuum does by no means have to be identical or even similar to the observed GRB and afterglow emission. The pre-ejected tori could plausibly be the result of a common-envelope phase preceding the GRB event. All types of GRB models pertaining to the class of black-hole accretion-disk models, including the collapsar/hypernova and the He-merger (see, e.g., Fryer, Woosley & Hartman for a review) are likely to have undergone a common-envelope phase prior to the primary’s core collapse. The material ejected during such a common-envelope phase is expected to have a directed velocity of the order of the escape velocity from the secondary,  $v \sim \sqrt{2GM_{\text{sec}}/R_{\text{sec}}} \sim 6 \times 10^7 (m/r)^{1/2} \text{ cm s}^{-1}$ , where  $M_{\text{sec}} = m M_{\odot}$  and  $R_{\text{sec}} = r R_{\odot}$  are the secondary’s mass and radius. For a detailed discussion of the expected structure of pre-ejected disks / tori, see Böttcher & Fryer (2001) and references therein. In the collapsar/hypernova models, the delay between the ejection of the primary’s hydrogen envelope and the GRB may be as large as 100,000 years, although significant uncertainties about the actual delay time scale remain. Such a long delay would place the pre-ejected material at radii  $R \gg 10^{16} \text{ cm}$ , probably too large to be consistent with the observed time delays of the GRB X-ray emission line features.

Much smaller delays are expected in the He-merger scenario (Zhang & Fryer 2001) and the supranova model (Vietri & Stella 1998). In the He-merger model, time delays of a few hundred years to a few times 10,000 years may be typical, allowing for both nearby and distant reprocessor scenarios. The supranova model predicts delays of the order of the spin-down time scale of the supramassive neutron star,  $t_{\text{sd}} \sim 10 j_{0.6} \omega_4^{-4} B_{12}^{-2} \text{ yr}$ , where  $j_{0.6}$  is the angular-momentum parameter in units of 0.6,  $\omega_4$  is the angular velocity

in units of  $10^4 \text{ s}^{-1}$ , and  $B_{12}$  is the surface magnetic field in units of  $10^{12} \text{ G}$ . Since the typical magnetic field strength is very poorly constrained, delays of several months to several thousands of years might be possible for this model. The ejecta velocity in this case should be more typical of supernova ejecta,  $v \sim 10^9 \text{ cm s}^{-1}$ . Thus it appears that the supranova model may be able to accommodate both distant and nearby reprocessor models as well as the thermal models discussed in the following section.

Different geometrical variations of distant reprocessor models have been discussed in more detail by Lazzati et al. (2000) and Vietri et al. (2001). Analytical estimates as well as detailed numerical simulations of distant reprocessor scenarios (e.g., Böttcher 2000, Weth et al. 2000) seem to converge to a mass requirement of  $M_{\text{Fe}} \sim 10^{-5} - 10^{-4} M_{\odot}$  for most of the observed Fe K $\alpha$  emission line features observed to date. Note, however, that Vietri et al. (2001) derive a significantly higher mass estimate of  $M_{\text{Fe}} \sim 1 M_{\odot}$  for GRB 991216, the most extreme case in terms of total energy emitted in the Fe K $\alpha$  line.

### Nearby Reprocessor Models

Nearby reproducers, at typical distances of  $\lesssim 10^{13} \text{ cm}$ , can either consist of pre-GRB ejecta (see discussion above) or the expanding envelope of a super-giant GRB progenitor (e.g., Rees & Mészáros 2000, McLaughlin et al. 2002). In the latter case, if the energy release in the GRB is strongly beamed, the envelope of the progenitor star is expected to remain in a quasi-stable state for a time of the order of the sound-crossing time through the progenitor,  $t_{\text{sc}} \sim 30 m_1^{-1/2} R_{13}^{3/2} \text{ d}$ , where  $m_1$  is the progenitor mass in units of  $10 M_{\odot}$ , and  $R_{13}$  is its radius in units of  $10^{13} \text{ cm}$ . It can thus plausibly survive the break-through of an ultrarelativistic jet, and provide a scattering funnel for persistent ionizing radiation throughout the prompt and early afterglow phase of the GRB.

In this class of models, the highly collimated ultrarelativistic outflow, most probably associated with the prompt GRB and the continuum afterglow emission, has moved far past the nearby reprocessor and can obviously not contribute to the illuminating continuum. Thus, these models require a persistent source of ionizing radiation over at least the duration over which the iron line is observed. Rees & Mészáros (2000) suggest that such a source could be provided by the gradually decaying energy flux from a magnetically driven relativistic wind from a fast-rotating, strongly magnetized neutron star (magnetar), if the primary GRB mechanism does not result in the formation of a black hole. They arrive at a required mass of  $M_{\text{Fe}} \sim 10^{-8} M_{\odot}$  of iron in a very thin, ionized skin of the funnel in order to reproduce an iron line with properties as observed in GRB 991216. However, if a similar abundance of iron is distributed throughout the entire stellar envelope, then a mass estimate more in line with the distant reprocessor models ( $M_{\text{Fe}} \sim 10^{-5} - 10^{-4} M_{\odot}$ ) results.

These estimates could be reduced if the line emission originates in a dense medium with relativistic electron densities of  $n_{e,rel} \sim 10^{10} - 10^{11} \text{ cm}^{-3}$ . In such an environment, the line emission could be enhanced by the Čerenkov effect, as recently pointed out by Wang et al. (2002). Another variation of nearby reprocessor models has recently been proposed by Kumar & Narayan (2002). They suggest the formation of a scattering screen at a distance of  $\sim 10^{14} - 10^{15} \text{ cm}$  from the GRB source, possibly as a result of  $\gamma\gamma$  pair creation on back-scattered GRB radiation. GRB emission from later (internal) shocks traveling along the jetted ejecta, are scattered back onto the outside of the stellar envelope of the progenitor (the supernova ejecta), and thus provide the ionizing flux for fluorescence line emission. This model requires a smaller iron content in the ejecta than previous models since it utilizes a larger fraction of the surface area of the progenitor's stellar envelope. Kumar & Narayan (2002) discuss this model in particular in light of the low-Z emission lines in GRB 011211 (Reeves et al. 2002). In this specific case, their model would require a relatively large pre-GRB outflow rate, producing a density in the surrounding medium of  $n_0 \sim 7 \times 10^7 \text{ cm}^{-3}$ , leading to an external-shock deceleration radius of  $r_{\text{dec}} \lesssim 5 \times 10^{14} \text{ cm}$ . This would correspond to an observed deceleration time scale of  $t_{\text{dec}} \lesssim 0.8 \Gamma_2^{-2} \text{ s}$ , which seems to be in conflict with the duration of  $t_{\text{dur}} \sim 270 \text{ s}$  of GRB 011211, with no indication of rapid variability on the time scale of the order of  $t_{\text{dec}}$ .

### THERMAL MODELS

As an alternative to photoionization models, Vietri et al. (1999) had suggested a thermal model in the framework of the supranova model. They argue that a relativistic fireball associated with the GRB might hit the pre-GRB supernova remnant within  $\sim 10^3 \text{ s}$  and heat the ejecta to  $T \sim 3 \times 10^7 \text{ K}$ . At such temperatures, the plasma emission is expected to show strong thermal bremsstrahlung emission as well as

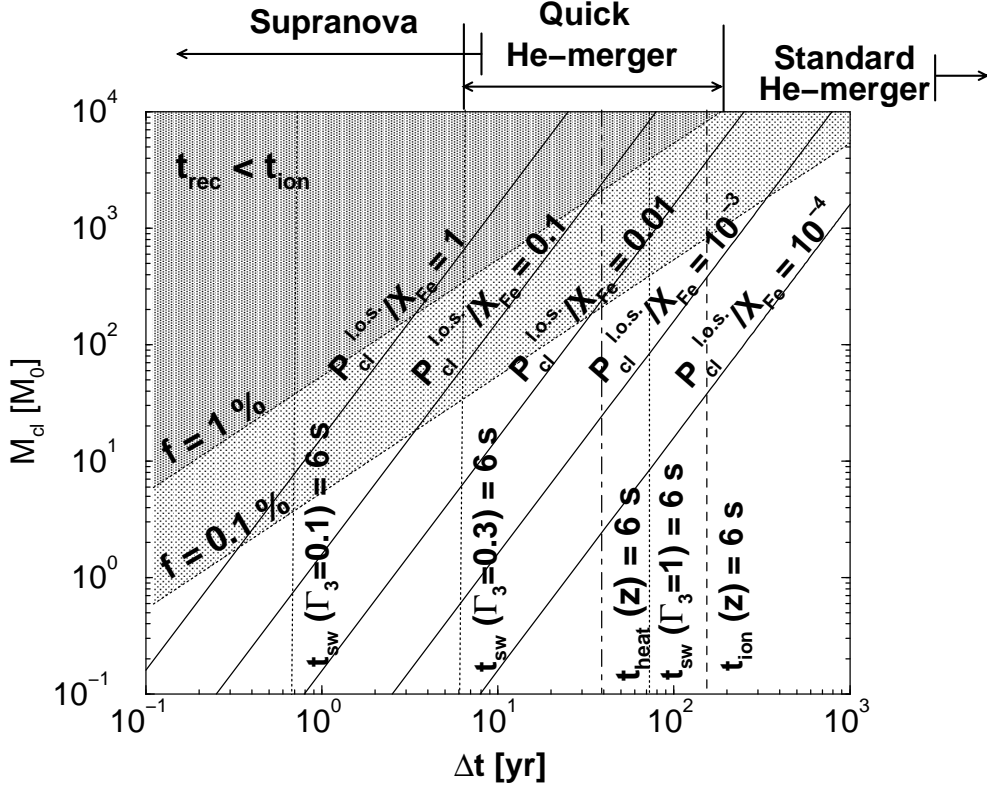


Fig. 2. Parameter constraints concerning supernova ejecta mass  $M_{\text{cl}}$  concentrated in dense clumps, and time delay  $\Delta t$  between the primary's supernova explosion and the GRB. Solid lines indicate the condition that an Fe K absorption edge of the depth observed in GRB 990705 is produced for various values of the ratio of the probability  $P_{\text{cl}}^{\text{l.o.s.}}$  of an absorbing cloud being located in the line of sight, to the iron enhancement,  $X_{\text{Fe}}$ , with respect to standard solar system values. Constellations which would give a consistent physical scenario must either be located close to the vertical line corresponding to  $t_{\text{ion}}(z) = 6$  s (if recombination is inefficient) or within the shaded regions in the upper left corner of the plot, which indicates the condition  $t_{\text{rec}} \leq t_{\text{ion}}$  for volume-filling factors of the SN ejecta of 1 % and 0.1 %, respectively, 1 year after the SN.

line emission, in particular strong Fe  $K\alpha$  recombination line emission. They suggest that the bremsstrahlung and recombination continuum may explain the secondary X-ray outburst observed in GRB 970508. Since the supranova model seems to be consistent with a large range of SN – GRB delays, one might expect that secondary X-ray outbursts and delayed X-ray emission line features on a variety of time scales can be explained with this type of models. General constraints on thermal emission scenarios for Fe  $K\alpha$  lines have also been considered by Lazzati et al. (1999).

Böttcher & Fryer have investigated the thermal X-ray emission from shock-heated pre-ejected material in alternative progenitor models (i.e. other than the supranova model), such as the collapsar/hypernova and the He-merger model. They found that the He-merger scenario provides a feasible setting for the production of transient Fe  $K\alpha$  line emission in the range of luminosities and durations observed. Since both the He-merger and the hypernova/collapsar models are also consistent with much larger SN – GRB delays, they predict that many GRBs may display late-time, thermal X-ray flashes from the shock-heating of pre-ejected material from a common-envelope phase, which could be detected out to redshifts of  $\sim 1$  with currently operating X-ray telescopes.

An alternative scenario based on thermal emission has recently been suggested by Mészáros & Rees (2001). As the collimated outflow from the central engine of a collapsar is piercing through the stellar envelope of the progenitor, a substantial amount of energy is deposited into the stellar material, which might be highly



magnetized. After the jet breaks out of the stellar envelope, this plasma bubble becomes buoyant and emerges through the evacuated funnel of the envelope within  $\sim 10^4 - 10^5$  s. At that time, it may have attained a temperature of  $\sim 10^6 - 10^7$  K, sufficient to produce iron lines, but potentially also a plasma emission spectrum dominated by lower-energy lines, as possibly observed in GRB 011211.

## MODEL IMPLICATIONS OF THE TRANSIENT ABSORPTION FEATURE

In principle, inferring constraints on parameters of the circumburst material from observed GRB properties is an easier task than inferring them from emission lines, because in the case of absorption features the continuum responsible for photoionization is identical to the observed GRB and afterglow continuum. Time-dependent X-ray absorption features had been studied for generic, quasi-homogeneous environments by Böttcher et al. (1999) and Ghisellini et al. (1999), and for more general cases, including radial gradients, by Lazzati et al. (2001) and Lazzati & Perna (2002). For given values of the depth  $\tau_{\text{edge}}$  of an absorption edge and the time scale  $t_{\text{edge}}$  within which it is disappearing, one can directly infer a characteristic radius (by setting  $t_{\text{ion}} = t_{\text{edge}}$ ). Combined with the column density derived from  $\tau_{\text{line}}$ , this allows a direct estimate of the (isotropic) amount of iron in the absorber.

It came as a big surprise that these estimates, applied to the parameters of the transient absorption line in GRB 990705 (Amati et al. 2000), yielded an estimate of  $M_{\text{Fe}} \sim 44 \Omega M_{\odot}$  within  $R \lesssim 1.3$  pc, where  $\Omega$  is the solid angle covered by the absorber as seen from the GRB source. Since this does obviously not seem realistic in any known astrophysical setting, additional effects due to clumping of the absorber in small clouds, in which recombination would become efficient (e.g., Böttcher et al. 2001), or resonance scattering of the Fe XXVI Ly $\alpha$  line out of the line of sight (Lazzati et al. 2001) had been considered. Both of these effects could plausibly reduce the necessary amount of iron in the absorber to  $M_{\text{Fe}} \lesssim 1 M_{\odot}$ , but require a rather extreme degree of clumping, with densities of  $n \sim 10^{11} \text{ cm}^{-3}$  in the clumps and distance/size ratios of  $x/r \sim 10^3 - 10^5$ .

Böttcher et al. (2002) have scaled the required parameters of the absorber to the clumping properties of supernova ejecta, derived from detailed 3-D hydrodynamics simulations of supernovae. The results were parameterized in terms of the total mass contained in the dense absorbing clouds,  $M_{\text{cl}}$ , and the time delay  $\Delta t$  between the supernova producing the absorbing ejecta, and the GRB. In the case of a supranova scenario,  $\Delta t$  is the delay between the progenitor supernova and the GRB, while in the He-merger scenario,  $\Delta t$  represents the time between the primary's supernova explosion and the He-merger-triggered GRB. Other progenitor models, such as the collapsar/hypernova models, would possess too dilute environments in order to be consistent with the observed properties of GRB 990705. The results of Böttcher et al. (2002) are summarized in Fig. 2, and illustrate that all currently discussed GRB models seem to be hard-pressed in order to produce the required environments to reproduce the transient absorption feature in GRB 990705, with the possible exception of the supranova scenario.

## REFERENCES

- Amati, L., et al., Discovery of a transient absorption edge in the X-ray spectrum of GRB 990705, *Science*, **290**, Issue 5493, 953, 2000.
- Antonelli, L. A., et al., Discovery of a redshifted iron K line in the X-ray afterglow of GRB 000214, *ApJ*, **545**, L39, 2000.
- Ballantyne, D. R., & Ramirez-Ruiz, Iron K $\alpha$  emission from X-ray reflection: Predictions for gamma-ray burst models *ApJ*, **559**, L83, 2001.
- Böttcher, M., et al., Time-dependent photoelectric absorption, photoionization and fluorescence line emission in gamma-ray burst environments, *A&A*, **343**, 111, 1999.
- Böttcher, M., Line emission from gamma-ray burst environments, *ApJ*, **539**, 102, 2000.
- Böttcher, M., and Fryer, C. L., X-ray spectral features from gamma-ray bursts: Predictions of progenitor models, *ApJ*, **547**, 338, 2001.
- Böttcher, M., et al., Implications of the transient absorption feature in GRB 990705, *AIP Conf. Proc.*, **587**, 190, 2001.
- Böttcher, M., Fryer, C. L., and Dermer, C. D., Transient absorption features in gamma-ray bursts and their implications for gamma-ray burst progenitors, *ApJ*, **567**, 441, 2002.
- Borozdin, K. N., and Trudolyubov, S. P., Observations of the X-ray afterglows of GRB 011211 and GRB 001025

- by XMM-Newton, *ApJ*, submitted (2002a).
- Dermer, C. D., Gamma ray bursts and cosmic ray origin, in *Proc. of XXVII ICRC*, 2001.
- Djorgowski, S. G., et al., The afterglow and the host galaxy of the dark burst GRB 970828, *ApJ*, **562**, 654, 2001.
- Fryer, C. L., Woosley, S. E., and Hartman, D. H., Formation rates of black hole accretion disk gamma-ray bursts, *ApJ*, **526**, 152, 1999.
- Ghisellini, G., et al., Redshift determination in the X-ray band of gamma-ray bursts, *ApJ*, **517**, 168, 1999.
- Ghisellini, G., et al., Emission lines in GRBs constrain the total energy reservoir, *A&A*, **389**, L33, 2002.
- Kallman, T. R., Mészáros, P., and Rees, M. J., Iron K lines from gamma-ray bursts, *ApJ*, submitted (2002).
- Kumar, P., and Narayan, R., X-ray lines from gamma-ray bursts *ApJ*, submitted (2002).
- Lazzati, D., et al., Iron line in the afterglow: A key to unveil gamma-ray burst progenitors, *MNRAS*, **304**, L31, 1999.
- Lazzati, D., et al., On the absorption feature in the prompt X-ray spectrum of GRB 990705, *ApJ*, **556**, 471, 2001.
- Lazzati, D., Perna, R., and Ghisellini, G., Time dependent photoionization opacities in dense gamma-ray burst environments, *MNRAS*, **325**, L19, 2001.
- Lazzati, D., and Perna, R., Determining the location of gamma-ray bursts through the evolution of their soft X-ray absorption, *MNRAS*, **330**, 383, 2002.
- Lazzati, D., Ramirez-Ruiz, E., & Rees, E., Soft X-ray emission lines in the early afterglow of gamma-ray bursts, *ApJ*, **572**, L57, 2002.
- McLaughlin, G. C., et al., Broad and shifted iron-group emission lines in gamma-ray bursts as tests of the hypernova scenario, *ApJ*, **567**, 454, 2002.
- McLaughlin, G. C., & Wijers, R. A. M. J., Delayed Nickel Decay in  $\gamma$ -ray bursts, *ApJ*, **580**, 1017, 2002.
- Mészáros, P., Theories of gamma-ray bursts, *Annual Review of Astronomy and Astrophysics*, **40**, 137, 2002.
- Mészáros, P., and Rees, M. J., The Edge of a gamma-ray burst afterglow, *MNRAS*, **299**, L10, 1998.
- Mészáros, P., and Rees, M. J., Collapsar jets, bubbles, and Fe lines, *ApJ*, **556**, L37, 2001.
- Paehrels, F., E. Kuulkers, J. Heise, and D. A. Liedahl, X-ray spectral diagnostics of gamma-ray burst environments, *ApJ*, **535**, L25, 2000.
- Perna, R., & Loeb, A., Identifying the environment and redshift of gamma-ray burst afterglows from the time dependence of their absorption spectra, *ApJ*, **501**, 467, 1998.
- Piro, L., et al., Iron line signatures in X-ray afterglows of GRBs by BeppoSAX, *A&AS*, **138**, 431, 1999.
- Piro, L., et al., Observation of X-ray lines from a gamma-ray burst (GRB 991216): Evidence of moving ejecta from the progenitor, *Science*, **290**, Issue 5493, 955, 2000.
- Rees, M. J., and Mészáros, P., Fe  $K\alpha$  emission from a decaying magnetar model of gamma-ray bursts *ApJ*, **545**, L73, 2000.
- Reeves, J. N., et al., The signature of supernova ejecta in the X-ray afterglow of the gamma-ray burst 011211, *Nature*, **416**, Issue 6880, 512, 2002a.
- Reeves, J. N., et al., Soft X-ray emission lines in the afterglow spectrum of GRB 011211: A detailed XMM-Newton analysis, *A&A*, submitted, 2002b.
- Vietri, M., and Stella, L., A gamma-ray burst model with small baryon contamination, *ApJ*, **507**, L45, 1998.
- Vietri, M., et al., On the anomalous X-ray afterglows of GRB 970508 and GRB 970828, *MNRAS*, **308**, L29, 1999.
- Wang, W., Zhao, Y., and You, J. H., Čerenkov line emission as a possible mechanism of X-ray lines in gamma-ray bursts, *ApJ*, **576**, L37, 2002.
- Yonetoku, D., et al., Nonequilibrium ionization states of gamma-ray burst environments, *ApJ*, **557**, L23, 2001.
- Yoshida, A., et al., What did ASCA see in the GRB 970828 afterglow?, *A&AS*, **138**, 433, 1999.
- Yoshida, A., et al., A possible emission feature in an X-ray afterglow of GRB 970828 as a radiative recombination edge, *ApJ*, **557**, L27, 2001.
- Zhang, W., and Fryer, C. L., The merger of a helium star and a black hole: gamma-ray bursts *ApJ*, **550**, 357, 2001.